



STABILITY OF ROTATION OF A MOTOR DRIVEN SHAFT ABOVE THE CRITICAL SPEED

J. ZAJĄCZKOWSKI

Lodz Technical University, Zwirki 36, Lodz, Poland

(Received 7 November 1996, and in final form 18 September 1997)

The paper is concerned with the problem of stability of a shaft driven by an electric motor. The behaviour of the system is explained by considering the motion on the energy surface. It is found that for the shaft with one end free to move axially, the energy surface has a minimum below the critical speed and a maximum above the critical speed. At resonance the energy surface is a slope plane. As the consequence of the shape of the energy surface, the motion above the critical speed is unstable and the speed of the shaft decreases to the critical value. For the shaft with ends kept a fixed distance apart, the local maximum on the energy surface is surrounded by an inclined concavity having a saddle and a global minimum. The local maximum and the saddle represent the states of unstable dynamic equilibrium. The global minimum represents the state in which the motion of the shaft above the critical speed is stable. The behaviour of the system disturbed from the unstable equilibrium states is demonstrated graphically.

© 1998 Academic Press Limited

1. INTRODUCTION

The problem of vibration of a rotating shaft has been studied by many authors. Only the papers that are directly related to the present study are cited here. The destabilizing effect of the internal damping on the motion of the shaft above the critical speed has been studied by Kimball [1], Ehrich [2] and Bucciarelli [3]. The problem of vibration of a beam with axially restrained ends has been investigated by van Dooren [4]. The constant speed motion of a shaft has been considered by Chang and Cheng [5] and Kurnik [6]. The motion of a shaft with a constant acceleration has been studied by Genta and Delprete [7]. This paper deals with the dynamics of the shaft for which the speed is a result of the interaction of the motor and the shaft.

2. EQUATIONS OF MOTION

The system considered, represented schematically in Figure 1, consists of a shaft, a rigid rotor of inertia B and a concentrated mass m . The rotor is driven by the motor torque M . The transverse displacement of the rotor B is prevented by bearings. The transverse displacement of the mass m results from the deflection of the shaft. The ends of the shaft can be restrained to remain a fixed distance apart. In this case the transverse deflection $r(x)$ is followed by the elongation of the shaft. To simplify the analysis, the continuously distributed mass of the shaft is not taken into account.

Taking the approximate deflection function in the form

$$r(x) = r \sin(\pi x/L) \quad (1)$$

the dependence of the stretching force N on the transverse deflection r can be found from

$$\Delta L = \int_0^L \frac{1}{2} \left(\frac{dr(x)}{dx} \right)^2 dx = \int_0^L \frac{N dx}{E_s A_s}, \quad (2)$$

where L is the length of the shaft, ΔL is the elongation of the shaft, E_s is the Young's modulus of elasticity and A_s is the area of the cross-section of the shaft. The dependence between the transverse concentrated force F applied at $x = x_F$ and the shaft deflection r can be found from the equation

$$\int_0^L r(x) \left(\frac{d^2}{dx^2} \left(E_s I_s \frac{d^2 r(x)}{dx^2} \right) - \frac{d}{dx} \left(N \frac{dr(x)}{dx} \right) - F \delta(x - x_F) \right) dx = 0, \quad (3)$$

where I_s is the moment of inertia of the cross-section of the shaft, $\delta(x)$ is a Dirac's delta function. For the force F applied at the centre of the shaft $x_F = L/2$, one obtains

$$F = (\pi^4/2)(E_s I_s/L^3)r + (\pi^4/8)(E_s A_s/L^3)r^3 = kr(1 + k_1 r^2). \quad (4)$$

For circular cross-section of a diameter d , the stiffness constants in equation (4) are found to be

$$k = (\pi^5/128)(E_s d^4/L^3), \quad k_1 = 4/d^2. \quad (5)$$

The motion of the considered system is governed by a set of non-linear ordinary differential equations

$$B \frac{d^2 \alpha}{dt^2} + c \frac{dv}{dt} (w_0 + w) - c \frac{dw}{dt} (v_0 + v) + kv(1 + k_1(v^2 + w^2))(w_0 + w) - kw(1 + k_1(v^2 + w^2))(v_0 + v) - M = 0,$$

$$\frac{d^2 v}{dt^2} - 2 \frac{d\alpha}{dt} \frac{dw}{dt} - \frac{d^2 \alpha}{dt^2} (w_0 + w) - \left(\frac{d\alpha}{dt} \right)^2 (v_0 + v) + \frac{c}{m} \frac{dv}{dt} + \frac{k}{m} (1 + k_1(v^2 + w^2))v = 0,$$

$$\frac{d^2 w}{dt^2} + 2 \frac{d\alpha}{dt} \frac{dv}{dt} + \frac{d^2 \alpha}{dt^2} (v_0 + v) - \left(\frac{d\alpha}{dt} \right)^2 (w_0 + w) + \frac{c}{m} \frac{dw}{dt} + \frac{k}{m} (1 + k_1(v^2 + w^2))w = 0. \quad (6)$$

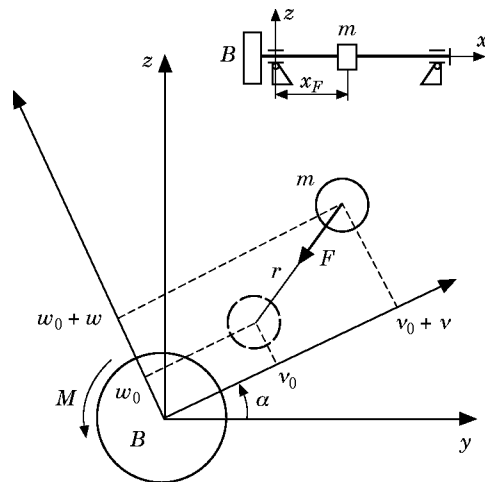


Figure 1. The shaft with ends restrained.

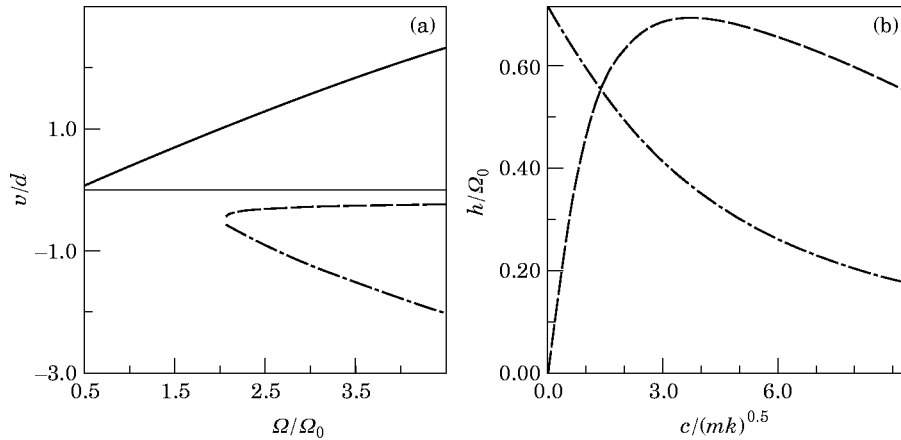


Figure 2. Equilibrium states of the shaft with ends kept a fixed distance apart for the stiffness $k_1 d^2 = 4$ and the eccentricity $v_0/d = 0.25$. (a) The dependence of the deflection on the angular speed of the shaft; (b) the dependence of the positive real parts of the eigenvalues of the stability matrix on the damping coefficient for $\Omega/\Omega_0 = 3$. —, For stable v (attractor); - - -, for unstable v (repellor) and corresponding h ; - · - · -, for unstable v (saddle) and corresponding h .

Here, v and w are the components of the displacement r of the mass m in the co-ordinate system fixed to the rotor B ; co-ordinates w_0 and v_0 define the static eccentricity of the mass m ; α is the rotation angle of the rotor; c is the coefficient of the internal damping.

The driving torque M can be found from the equation

$$T_m \frac{dM}{dt} = C_m (\Omega_m - d\alpha/dt) - M \tag{7}$$

where T_m is a time constant of the motor, C_m is slope of the static characteristic of the motor and Ω_m is a speed of the motor for which the static moment is equal to zero.

3. THE STATE OF DYNAMIC EQUILIBRIUM

The dynamic equilibrium state solution can be found by substituting the driving moment and the velocities

$$M = 0, \quad \Omega = d\alpha/dt = \Omega_m, \quad dv/dt = 0, \quad dw/dt = 0, \tag{8}$$

into the set of equations (6, 7). The resulting equations

$$-\Omega^2 m(v_0 + v) + k(1 + k_1(v^2 + w^2))v = 0, \quad -\Omega^2 m(w_0 + w) + k(1 + k_1(v^2 + w^2))w = 0, \tag{9}$$

determine the deflection of the motor driven shaft. The equations (9) are the same as for the shaft rotating with a constant speed [5]. The equilibrium state solutions found from equations (9) are shown in Figure 2a in the parameter space of Ω/Ω_0 for $\Omega_0 = (k/m)^{1/2}$, $w_0 = 0$, $v_0/d = 0.25$ and $k_1 d^2 = 4$.

It is convenient to rewrite the set of equations (6, 7) in the general form

$$\mathbf{F}(\mathbf{X}) = 0, \quad \mathbf{X} = \left[\frac{dM}{dt}, M, \frac{d^2\alpha}{dt^2}, \frac{d\alpha}{dt}, \alpha, \frac{d^2v}{dt^2}, \frac{dv}{dt}, v, \frac{d^2w}{dt^2}, \frac{dw}{dt}, w \right]. \tag{10}$$

Designating by $\delta\xi$ the disturbance from the equilibrium state ξ , taking the disturbed solution in the form

$$\mathbf{X}(t) = \xi(t) + \delta\xi(t). \quad (11)$$

and applying Taylor's expansion to equation (10), the stability equation can be written as follows

$$\mathbf{F}_n(\mathbf{X}) = \mathbf{F}_n(\xi) + \frac{\partial \mathbf{F}_n(\xi)}{\partial \xi_1} \delta\xi_1 + \frac{\partial \mathbf{F}_n(\xi)}{\partial \xi_2} \delta\xi_2 + \frac{\partial \mathbf{F}_n(\xi)}{\partial \xi_3} \delta\xi_3 + \dots \quad (12)$$

Here, $\mathbf{F}(\mathbf{X}) = 0$ and $\mathbf{F}(\xi) = 0$.

Applying formula (12) to the set of equations (6,7), one obtains

$$d\delta M/dt = -(1/T_m)(C_m d\delta\alpha/dt + \delta M),$$

$$\begin{aligned} & B d^2\delta\alpha/dt^2 + c(w_0 + w) d\delta v/dt - c(v_0 + v) \frac{d\delta w}{dt} - \delta M \\ & + (-cdw/dt + k(w_0 + w)(1 + 3k_1v^2) + kk_1(w_0 + w)w^2 - kw(1 + k_1w^2) \\ & - kk_1vw(2v_0 + 3v))\delta v + (c dv/dt - k(v_0 + v)(1 + 3k_1w^2) \\ & - kk_1(v_0 + v)v^2 + kv(1 + k_1v^2) + kk_1vw(2w_0 + 3w))\delta w = 0, \end{aligned}$$

$$\begin{aligned} & \frac{d^2\delta v}{dt^2} - (w_0 + w) \frac{d^2\delta\alpha}{dt^2} - 2\left(\frac{dw}{dt} + (v_0 + v) \frac{d\alpha}{dt}\right) \frac{d\delta\alpha}{dt} - 2 \frac{d\alpha}{dt} \frac{d\delta w}{dt} + \frac{c}{m} \frac{d\delta v}{dt} \\ & + \left(-\left(\frac{d\alpha}{dt}\right)^2 + \frac{k}{m} (1 + 3k_1v^2) + \frac{kk_1}{m} w^2\right)\delta v + \left(-\frac{d^2\alpha}{dt^2} + 2 \frac{kk_1}{m} vw\right)\delta w = 0, \end{aligned}$$

$$\begin{aligned} & \frac{d^2\delta w}{dt^2} + (v_0 + v) \frac{d^2\delta\alpha}{dt^2} + 2\left(\frac{dv}{dt} - (w_0 + w) \frac{d\alpha}{dt}\right) \frac{d\delta\alpha}{dt} + 2 \frac{d\alpha}{dt} \frac{d\delta v}{dt} + \frac{c}{m} \frac{d\delta w}{dt} \\ & + \left(-\left(\frac{d\alpha}{dt}\right)^2 + \frac{k}{m} (1 + 3k_1w^2) + \frac{kk_1}{m} v^2\right)\delta w + \left(\frac{d^2\alpha}{dt^2} + 2 \frac{kk_1}{m} vw\right)\delta v = 0, \end{aligned}$$

The set of equations (13) can be rewritten as a set of first order differential equations

$$(d/dt)\delta\mathbf{U} = \mathbf{D}(\mathbf{U})\delta\mathbf{U} \quad (14)$$

where $\mathbf{U} = [M, \alpha, v, w, d\alpha/dt, dv/dt, dw/dt]^T$ and $\delta\mathbf{U} = [\delta M, \delta\alpha, \delta v, \delta w, d\delta\alpha/dt, d\delta v/dt, d\delta w/dt]^T$. The eigenvalues of the stability matrix \mathbf{D} were calculated for the equilibrium solutions defined by equations (9) (shown in Figure 2a) for $w_0 = 0$, $v_0/d = 0.25$, $k_1d^2 = 4$, $B/(md^2) = 20$, $C_m/(md^2\Omega_0) = 10$, $\Omega_0 = (k/m)^{1/2}$, $T_m\Omega_0 = 1$, $\Omega/\Omega_0 = 3$. The positive real parts of the eigenvalues h/Ω_0 versus the damping coefficient $c/(mk)^{1/2}$ are plotted in Figure 2b. The real part of the eigenvalue corresponding to the stable equilibrium state represented by the solid line in Figure 2a is negative and it is not shown in Figure 2b.

To illustrate the stability of the system the energy E associated with the dynamic equilibrium state is defined as a potential

$$\begin{aligned} \partial E / \partial v &= F_v, & \partial E / \partial w &= F_w, \\ F_v &= k(1 + k_1(v^2 + w^2))v - \Omega^2 m(v_0 + v), \\ F_w &= k(1 + k_1(v^2 + w^2))w - \Omega^2 m(w_0 + w). \end{aligned} \tag{15}$$

The forces F_v and F_w (9, 15) represent the elastic reaction of the shaft decreased by the centrifugal force. The energy is found to be of the form

$$E = k([v^2 + w^2]/2 + (k_1/4)(v^2 + w^2)^2) - (m\Omega^3/2)((v_0 + v)^2 + (w_0 + w)^2). \tag{16}$$

The cross-sections of the energy surface E/k versus v/d and E/k versus w/d for the shaft having one end free to move axially ($k_1 = 0$) with the static eccentricity $v_0/d = 0.25$ are shown in Figure 3a for $\Omega/\Omega_0 = 0.2$, Figure 3b for $\Omega/\Omega_0 = 1$ and Figure 3c for $\Omega/\Omega_0 = 3$. It can be seen that the shape of the energy surface changes with the increase of the angular speed. For the speed lower than the critical one the energy surface has a minimum. It becomes a slope plane at the resonance. Over the critical speed the energy surface has a maximum.

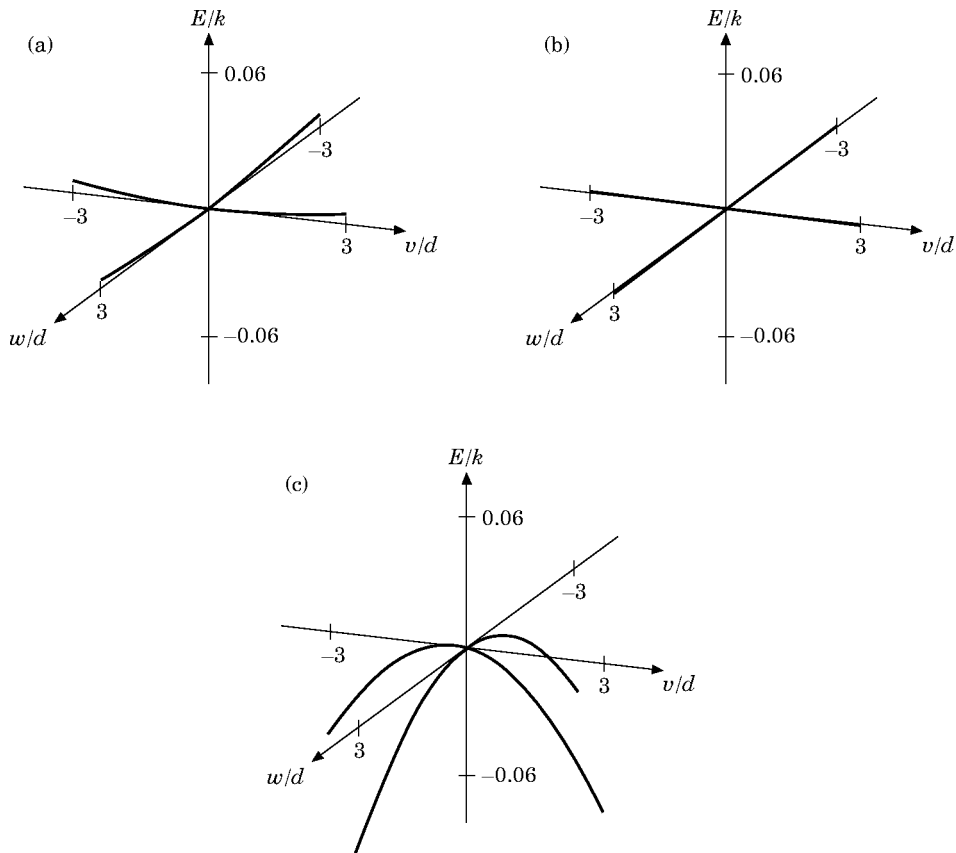


Figure 3. The cross-sections of the energy surface E/k versus v/d and E/k versus w/d for the shaft having one end free to move axially ($k_1 = 0, v_0/d = 0.25$); (a) below the critical speed $\Omega/\Omega_0 = 0.2$; (b) at the critical speed $\Omega/\Omega_0 = 1$; (c) above the critical speed $\Omega/\Omega_0 = 3$.

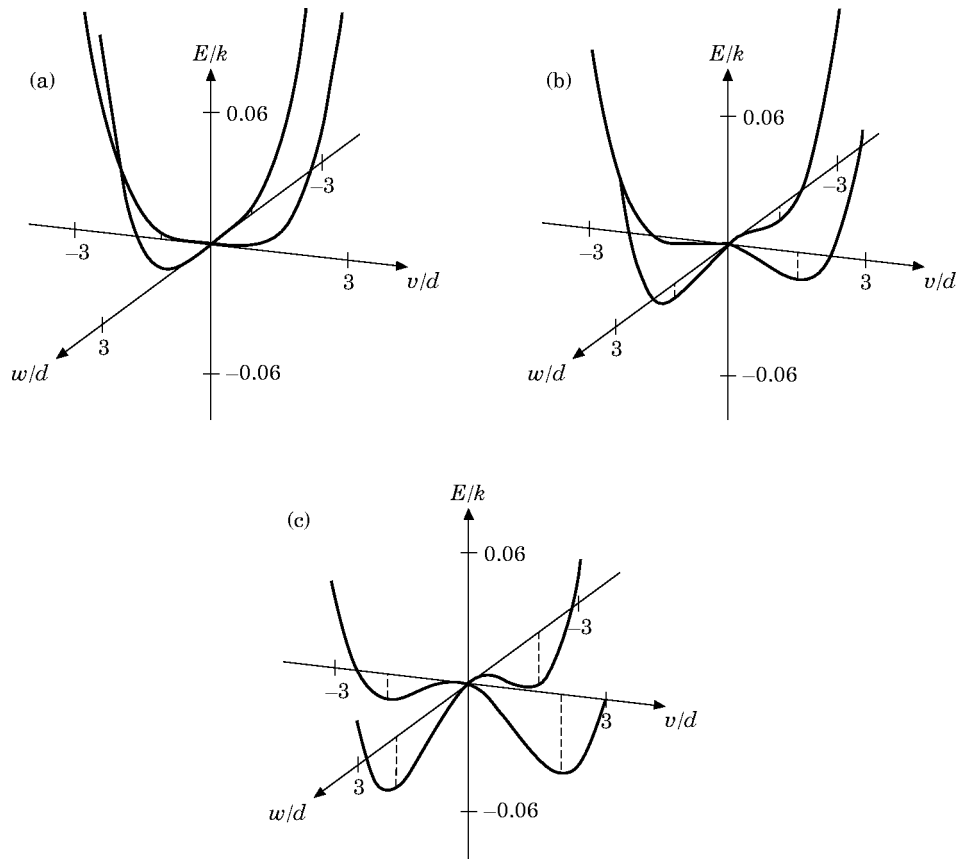


Figure 4. The cross-sections of the energy surface E/k versus v/d and E/k versus w/d for the shaft with ends kept fixed distance apart ($k_1 d^2 = 4$, $v_0/d = 0.25$): (a) below the critical speed $\Omega/\Omega_0 = 0.2$; (b) above the critical speed for $\Omega/\Omega_0 = 3$; (c) $\Omega/\Omega_0 = 4$.

The cross-sections of the energy surface E/k versus v/d and E/k versus w/d for the shaft with ends kept fixed distance apart ($k_1 d^2 = 4$) with the static eccentricity $v_0/d = 0.25$ are shown in Figure 4a for $\Omega/\Omega_0 = 0.5$, Figure 4b for $\Omega/\Omega_0 = 3$ and Figure 4c for $\Omega/\Omega_0 = 4$. It can be seen that for the speed higher than the critical one the energy surface has a local maximum surrounded by an inclined concavity. The concavity has a saddle point and a global minimum. The maximum corresponds to the unstable equilibrium state represented by the dashed line in Figure 2a. The saddle point corresponds to the unstable equilibrium state represented by the dashdot line in Figure 2a. The global minimum corresponds to the stable dynamic equilibrium state represented by the solid line in Figure 2a.

In order to observe the behaviour of the system disturbed from the state of dynamic equilibrium the set of equation (6, 7) was numerically integrated for the initial conditions corresponding to the solution (9) with the initial disturbance $\delta v = 0.01v$ taking $\Omega_m/\Omega_0 = 3$, $w_0 = 0$, $v_0/d = 0.25$, $B/(md^2) = 20$, $c/(mk)^{1/2} = 0.1$, $C_m/(md^2\Omega_0) = 10$, $\Omega_0 = (k/m)^{1/2}$ and $T_m\Omega_0 = 1$.

The behaviour of the shaft having one end free to move axially ($k_1 = 0$), disturbed from the energy maximum, is shown in Figure 5. It can be seen that the system leaves the state of equilibrium. The trajectory v versus w is an outward spiral. The angular speed of the shaft decreases to the critical value. The decrease of the shaft speed results in the decrease of the curvature of the energy surface. It changes from the convexity shown

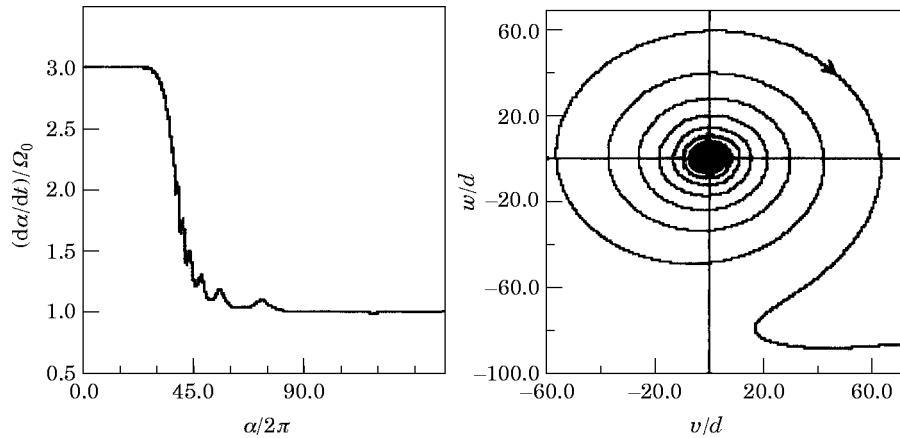


Figure 5. The angular velocity and the transverse deflection of the shaft having one end free to move axially ($k_1 = 0$) and disturbed from the unstable equilibrium state for $v_0/d = 0.25$ and $\Omega_m/\Omega_0 = 3$.

in Figure 3c to the slope plane shown in Figure 3b. The motion is then continued on that plane.

The behaviour of the shaft with ends kept fixed distance apart ($k_1 d^2 = 4$) disturbed from the local energy maximum is shown in Figure 6. It can be seen that the system leaves the state of equilibrium. The motion of the system starts with an outward spiral at the energy maximum and it ends with an inward spiral at the energy minimum. There are some instantaneous speed variations during the transition period and they have some influence on the shape of energy surface. At the energy minimum the shaft speed over the critical value, is maintained.

The calculations performed for both the linear and non-linear systems have shown that the increase in the stiffness of the motor characteristics C_m or the inertia B of the rotor did not prevent the instability at the energy maximum. On the other hand, in the absence of internal damping the system stayed at the maximum. This is because in this case the real part of the corresponding eigenvalue of the stability matrix is equal to zero (dashed line in Figure 2b).

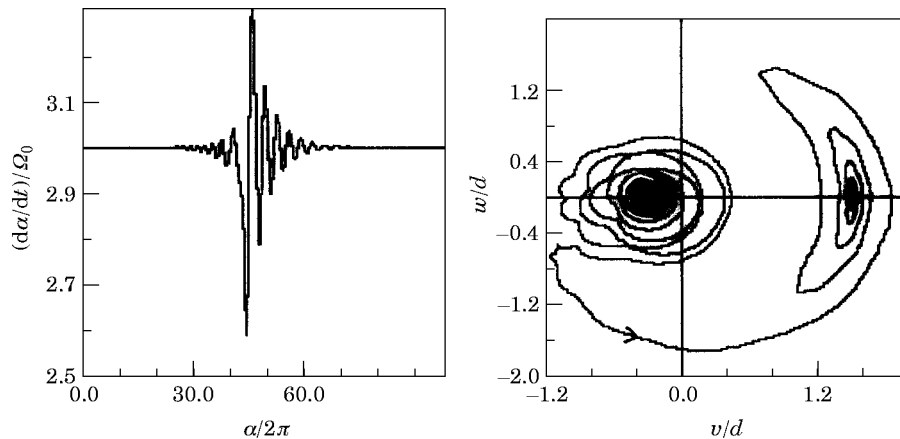


Figure 6. The angular velocity and the transverse deflection of the shaft with ends kept fixed distance apart and disturbed from the unstable equilibrium state represented by local energy maximum for $k_1 d^2 = 4$, $v_0/d = 0.25$ and $\Omega_m/\Omega_0 = 3$.

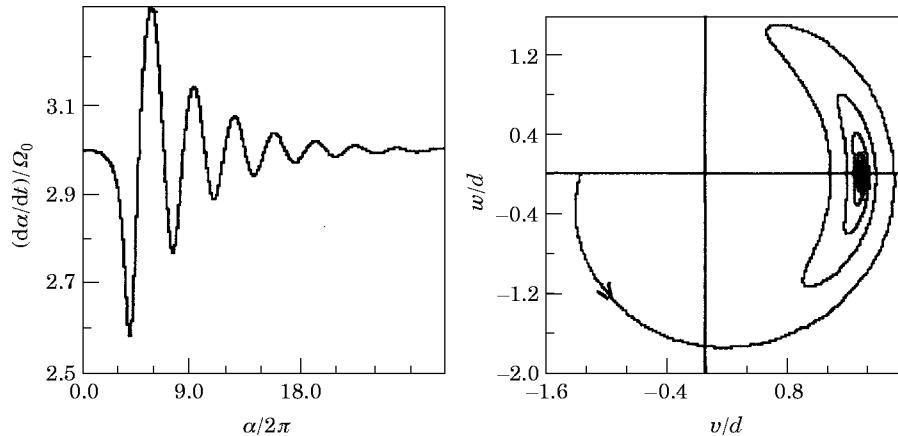


Figure 7. The angular velocity and the transverse deflection of the shaft with ends kept fixed distance apart and disturbed from the unstable equilibrium state represented by the saddle on the energy surface for $k_1 d^2 = 4$, $v_0/d = 0.25$ and $\Omega_m/\Omega_0 = 3$.

The behaviour of the shaft with ends kept fixed distance apart ($k_1 d^2 = 4$) disturbed from the saddle point on the energy surface is shown in Figure 7. The system leaves the state of equilibrium. The trajectory v versus w goes around on the energy surface and as it approaches the energy minimum, it becomes an inward spiral. The speed variations during the transition period have some influence on the shape of the energy surface. At the energy minimum the shaft speed over critical value is maintained. The described behaviour was also observed when the internal damping was absent. This is because the real part of the corresponding eigenvalue of the stability matrix is not equal to zero (dashdot line in Figure 2b).

4. CONCLUDING REMARKS

If the shaft has one end free to move axially then the energy surface has a minimum below the critical speed and a maximum above the critical speed. It is a slope plane at the resonance. If internal damping is present then the motion above the critical speed leads to the decrease of the shaft speed to the critical value.

If the shaft has its ends kept a fixed distance apart then, above the critical speed, the maximum on the energy surface is surrounded by a inclined concavity having a saddle and a global minimum. The global minimum represents the state of stable rotation of the shaft with the speed higher then the critical one. The saddle represents the state of unstable rotation of the shaft. The maximum represents the unstable rotation of the shaft if the internal damping is present. The system disturbed from those two unstable states goes to the energy minimum. If the internal damping is absent then at the energy maximum the real part of the eigenvalue of the stability matrix is equal to zero. In this case the system can operate at the energy maximum.

REFERENCES

1. A. L. KIMBALL 1924 *General Electric Review* **17**, 244–251. Internal friction theory of shaft whipping.
2. F. F. EHRICH 1964 *Transactions of the American Society of Mechanical Engineers Journal of Applied Mechanics* **31**, 279–282. Shaft whirl induced by rotor internal damping.

3. L. L. BUCCIARELLI 1982 *Transactions of the American Society of Mechanical Engineers Journal of Applied Mechanics* **49**, 425–428. On the instability of rotating shaft due to internal damping.
4. R. VAN DOOREN 1975 *Journal of Sound and Vibration* **41**, 133–142. Vibrations of order $1/9$ of a non-linear beam forced by a two mode harmonic load.
5. C. O. CHANG and J. W. CHENG 1993 *Journal of Sound and Vibration* **160**, 433–456. Non-linear dynamics and instability of a rotating shaft–disk system.
6. W. KURNIK 1994 *Nonlinear Dynamics* **5**, 39–52. Stability and bifurcation analysis of a nonlinear transversally loaded rotating shaft.
7. G. GENTA and C. DELPRETE 1995 *Journal of Sound and Vibration* **180**, 369–386. Acceleration through critical speeds of an anisotropic non-linear, torsionally stiff rotor with many degrees.

APPENDIX: MAIN SYMBOLS

A_x	area of the cross-section of the shaft
B	mass moment of inertia of the rotor
c	internal damping constant
C_m	slope of the static characteristic of the motor
d	diameter of the cross-section of the shaft
\mathbf{D}	stability matrix
E	energy defined as a potential
E_s	Young's modulus of elasticity
F	transverse concentrated force
F_x, F_w	components of the elastic reaction of the shaft decreased by the centrifugal force
h	real part of the eigenvalue of the stability matrix \mathbf{D} ; Lyapunov exponent
I_s	moment of inertia of the cross-section of the shaft.
k, k_1	stiffness constants of the shaft
L	length of the shaft,
m	concentrated mass
M	motor torque
N	normal stretching force resulting from the elongation ΔL of the shaft
r	transverse displacement of the mass m in the rotating reference frame
T_m	time constant of a motor
\mathbf{U}	column matrix $[M, \alpha, v, w, d\alpha/dt, dv/dt, dw/dt]^T$
v, w	components of the displacement r of the mass m in the co-ordinate system fixed to the rotor
B	
v_0, w_0	static eccentricity of the mass m
\mathbf{X}	vector $\{dM/dt, M, d^2\alpha/dt^2, d\alpha/dt, \alpha, d^2v/dt^2, dv/dt, v, d^2w/dt^2, dw/dt, w\}$
x_F	co-ordinate of concentrated mass m and force F
α	rotation angle of the shaft
ΔL	elongation of the shaft resulting from its transverse deflection $r(x)$
$\delta(x)$	Dirac's delta function
$\delta\zeta$	disturbance of ζ
δv	disturbance of v
$\delta\mathbf{U}$	disturbance of \mathbf{U}
ζ	dynamic equilibrium state of X
Ω_m	speed of the motor for which the motor torque M is equal to zero for $T_m = 0$
Ω	angular velocity of the shaft
Ω_0	natural frequency of the flexural vibration of the shaft $\Omega_0 = (k/m)^{1/2}$